Int. J. Electrochem. Sci., 11 **(2016)** 250 - 258

International Journal of
ELECTROCHEMICAL
SCIENCE
www.electrochemsci.org

A Novel Tyrosinase Biosensor based on Graphene and Co_3O_4 Nanocomposite Materials for Rapid Determining Catechol

Kehong Liang[1‡], *Xiaochen Fu*[2‡], *Lidong Wu*[2,*], *Yuchang Qin*[1*], *Yi Song*[2]

[1] Institute of Food and Nutrition Development, Ministry of Agriculture, Beijing 100081, China
[2] Chinese Academy of Fishery Sciences, Beijing 100141, China
[‡]the authors contribute equally to this work.
[*]E-mail: wuld@cafs.ac.cn, liangkehong@caas.cn

Received: 19 August 2015 / *Accepted:* 28 September 2015 / *Published:* 1 December 2015

Based on graphene and Co_3O_4 nanocomposite (GP-Co_3O_4), a novel tyrosinase biosensor is constructed for rapid determining catechol. The results demonstrated that GP-Co_3O_4 modified tyrosinase biosensor possessed fantastic advantages over tyrosinase biosensor in sensitivity and limit of detection (LOD). This might be ascribed to the large specific surface area of graphene and spongy Co_3O_4. The GP-Co_3O_4 modified tyrosinase biosensor showed superb analytical performances, such as a linear range from 1 to 30 μmol L^{-1}, LOD of 30 nmol L^{-1}, and sensitivity of 1856.8 mA cm^{-2} M^{-1}. The tyrosinase biosensor was successfully utilized for detecting catechol, and proved to be a potential and reliable method for analysis emergency affairs of catechol on-site.

Keywords: Electrochemical biosensor; tyrosinase; rapid dectection; catechol

1. INTRODUCTION

Catechol (known as 1,2-dihydroxybenzene) is an organic compound which utilized as a common building block in organic synthesis. Catechol always exists naturally in trace level. When the catechol exposed to oxygen and catecholase, the colorless catechol oxidizes to reddish-brown derivatives of benzoquinose, such as transection of apple or potato. The rapid, on-site detection method for catechol is of significant importance in fruit monitoring. Without labor-consuming and complicated sample pretreatment, the electrochemical tyrosinase biosensor provides an excellent prospect for rapid monitoring catechol in fruit.

The immobilization nanomaterials serve as an important element in the development of enzyme biosensor. The excellent nanomaterial as biosensing platform is the key factor of enzyme biosensor for

improving limit of detection (LOD) and sensitivity, etc. In recent decades, carbon nanomaterial has been developed as enzyme-support nanomaterials, such as graphene [1-3], carbon nanotubes [4, 5], mesoporous carbon [6, 7] and fullerene [8-10]. Especially, graphene as a novel biosensing platform has triggered mounting interest owing to its high specific surface area, excellent electric conductivity, superb chemical and thermal stability, and toxicological safety, all of which make it attractive for the construction of electrochemical biosensor [11, 12].

Graphene is a monolayer of sp^2 hybridized carbon atoms, which packed into a dense honeycomb crystal structure [13]. Ye group had developed electrochemical glucose oxidase biosensor based on reduced graphene oxide, chitosan and gold nanoparticles for detecting of glucose with LOD of 0.52 μmol L^{-1} [14]. A novel electrochemical immunosensor based on graphene nanosheets was utilized for determining botulinum neurotoxin-E at trace level (LOD, 5.0 pg ml^{-1}), reported by Narayanan et al [1]. Many kinds of graphene modified biosensors were developed for monitoring pollution [15-18], biomolecules [2, 19, 20], toxicants [21-23] and so on [24].

The prepared graphene and Co_3O_4 nanocomposite (GP-Co_3O_4) was utilized as tyrosinase immobilization platform and glassy carbon (GC) electrode modification material to develop an electrochemical biosensor. Furthermore, the performances of GP-Co_3O_4 modified tyrosinase biosensor were systematically studied. The results demonstrated that this biosensor possessed higher sensitivity, lower LOD and background current than the biosensor only tyrosinase immobilization. It might fulfill the demand for the rapid and on-site determining of catechol in real fruit sample.

2. EXPERIMENTAL SECTION

2.1 Materials and Solutions.

Catechol, tyrosinase (from mushroom, >1000 units mg^{-1}, pI 5.92), chitosan (Chi) and other chemicals (analytical reagent grade) were purchased from Sigma Aldrich (USA). Millipore Milli-Q water (18 MΩ cm) was used as solvent in all experiments. Unless noted otherwise, 50 mmol L^{-1} pH 6.9 phosphate buffer solution (PBS) was used as the supporting electrolyte in all electrochemical experiments.

2.2. Apparatus

Electrochemical impedance spectroscopy (EIS), current–time curve (I–t) and cyclic voltammetry (CV) were performed on glassy carbon electrodes (GC, diameter 3 mm) using a CHI 660b Electrochemical Workstation (Shanghai, China). The electrochemical measurements were carried on a three-electrode system with the GP-Co_3O_4 modified GC electrode as the working electrode, Ag/AgCl as the reference electrode (KCl concentration: 3 mol L^{-1}), and a platinum wire as the auxiliary electrode. Transmission electron microscopy (TEM) images were obtained by a JEM-2100 (Japan).

2.3. Graphene-Co_3O_4 modification of GC electrode

Graphene was prepared by a ball-milling method reported by previous study [25]. And Co_3O_4 nanoflakes were obtained according to the method reported by Lu group [26]. The surface of GC electrode was polished by alumina powder (0.05 μm) and washed ultrasonically by Milli-Q water. Then, 5 μL 0.8 mg mL^{-1} graphene solution, 5 μL 1.0 mg mL^{-1} Co_3O_4 solution, 5 μL of Chi (6 mg mL^{-1}) and 5 μL Milli-Q water became homogeneous mixture by ultrasonic oscillating. Subsequently, 5 μL mixture was dropped onto the GC electrode and obtain a GP-Co_3O_4-Chi-Tyr/GC electrode. This electrode stored in a refrigerator at 4℃ until in use. Other enzyme electrodes were developed in the same procedures as described above.

2.3. Procedure for I-t analysis by GC electrode

All of the I-t analysis was performed in 8 mL stirring PBS solution with a constant potential value of -0.1 V at room temperature with continual dropping of catechol. The response signal of catechol was monitored by the GP-Co_3O_4-Chi-Tyr/GC electrode.

3. RESULTS AND DISCUSSION

3.1. TEM and impedance spectroscopy characterization of Graphene-Co_3O_4 nanocomposite material

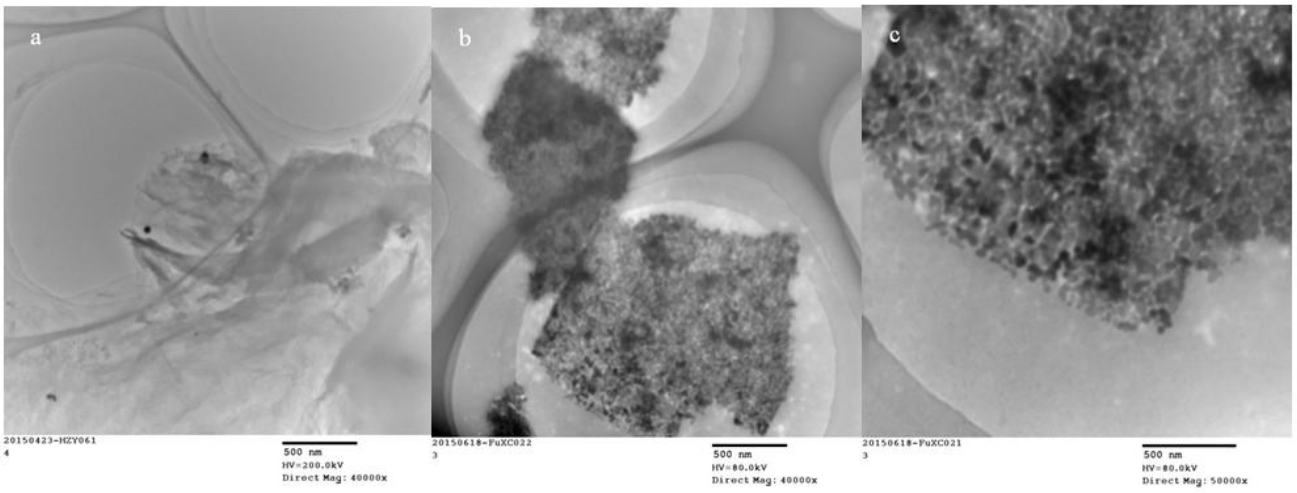

Figure 1. TEM images of a) graphene, b) Graphene-Co_3O_4 nanocomposite and c) the magnified image of Graphene-Co_3O_4.

Figure 1 showed the representative TEM images of graphene and Graphene-Co_3O_4 nanocomposite. The morphology of graphene which prepared by previous reported ball milling method was displayed in Figure 1a. The representative TEM image of Graphene-Co_3O_4 was shown in Figure 1b, and the magnified image of Graphene-Co_3O_4 was displayed in Figure 1c. It demonstrated that the

Co_3O_4 was distributed on the surface of graphene to obtain the Graphene-Co_3O_4 nanocomposite. Our previous study indicated that graphene with hierarchical nanostructure could immobilize enzyme molecules by its unique layer-by-layer self-assembly morphology. Introducing good hydrophilicity and biocompatibility Co_3O_4, the alliance between graphene and Co_3O_4 resulted in the formation of a novel nanocomposite. The nanocomposite could serve as an important role in the electron transfer between enzyme and the electrode surface.

As is well known, electrochemical impedance spectroscopy (EIS) is an effective technique to monitor the electron transfer changes of GC electrode surface film. The EIS plot consists of a linear portion and a semicircle portion. The semicircle portion occurs at high frequencies corresponding to the ability of electron transfer. The diameter of the semicircle portion equals to the charge-transfer resistance (Rct), which controls the electron-transfer kinetics of the redox probe at the electrode surface.

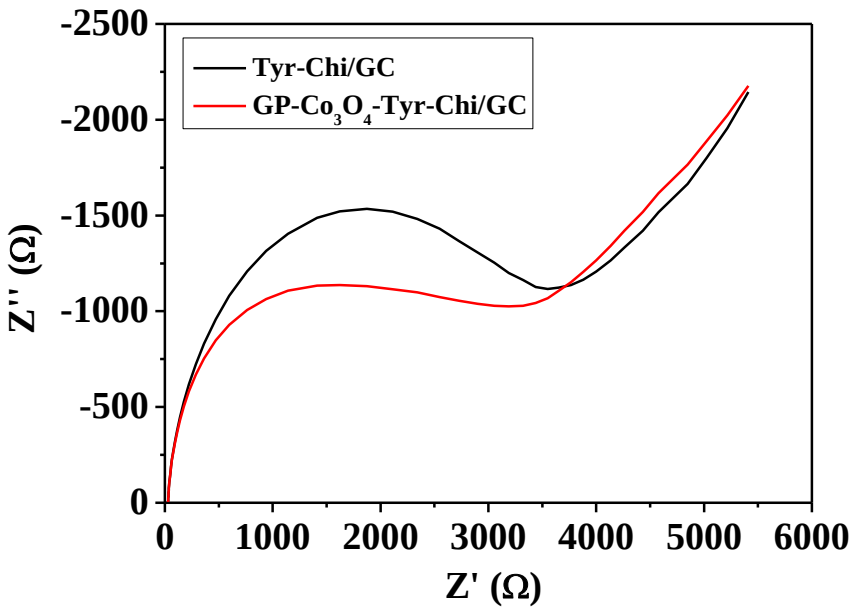

Figure 2. Nyquist plots of Tyr-Chi/GC and GP-Co_3O_4-Tyr-Chi/GC electrodes in 2 mmol L^{-1} $K_3Fe(CN)_6$ containing 0.5 mmol L^{-1} KNO_3.

The linear portion often generates at low frequencies corresponding to the diffusion process. In case of rapid electron transfer process, the Nyquist plot might only contain a linear portion. As shown in Figure 2, the diameter of semicircle for Tyr-Chi/GC electrode (3700 Ω) was larger than that of GP-Co_3O_4-Tyr-Chi/GC electrode (3000 Ω) in the 2 mmol L^{-1} $K_3[Fe(CN)_6]$ solution containing 0.5 mol L^{-1} KNO_3. After the introduction of Graphene-Co_3O_4 nanocomposite to modify the GC electrode, the diameter of semicircle decreased obviously. It demonstrated that Graphene-Co_3O_4 nanocomposite prompted the electron transfer between the redox probe of $[Fe(CN)_6]^{3-/4-}$ and the electrode surface film. The improved interface conductivity was attributed to the introduction of Graphene-Co_3O_4 nanocomposite.

3.2 Electrochemical characterization of GP-Co_3O_4-Tyr-Chi/GC electrode

For researching the direct electron transfer of tyrosinase immobilized on the GP-Co_3O_4 nanocomposite, cyclic voltammetry (CV) measurements were utilized in the 50 mmol L^{-1} N_2-saturated PBS (pH 6.9) at 100 mV s^{-1}. A pair of well-defined redox peaks was obtained on the GP-Co_3O_4-Tyr-Chi/GC electrode (Figure 3, black line), which was obviously larger than that of Tyr-Chi/GC electrode. This difference was mainly due to the fact that GP-Co_3O_4 nanocomposite could enhance direct electron transfer efficiency between the tyrosinase molecules and GC electrode.

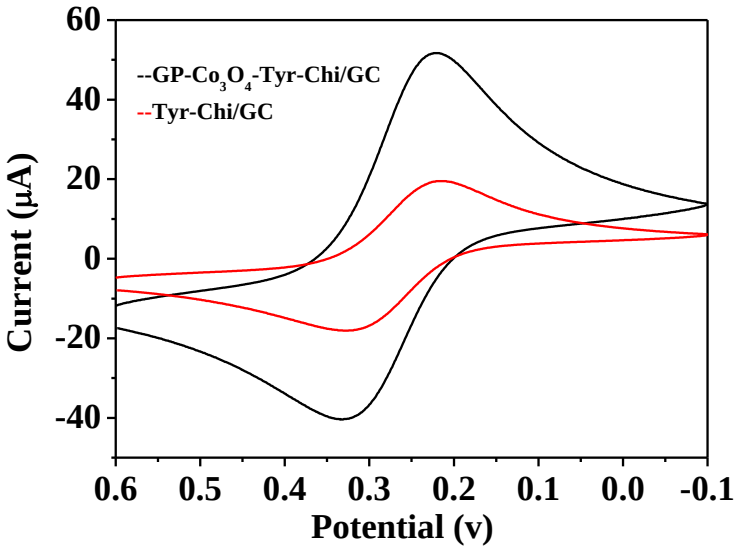

Figure 3. Cyclic voltammetry curves of Tyr-Chi/GC and GP-Co_3O_4-Tyr-Chi/GC electrodes in 50 mmol L^{-1} N_2-saturated PBS (pH 6.9).

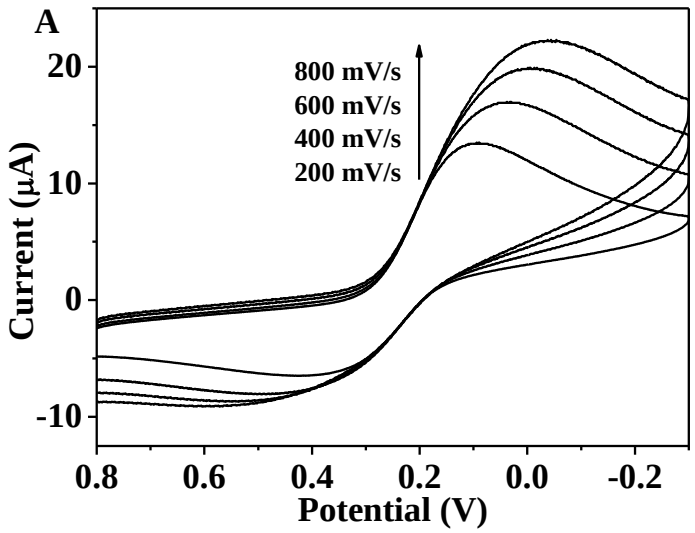

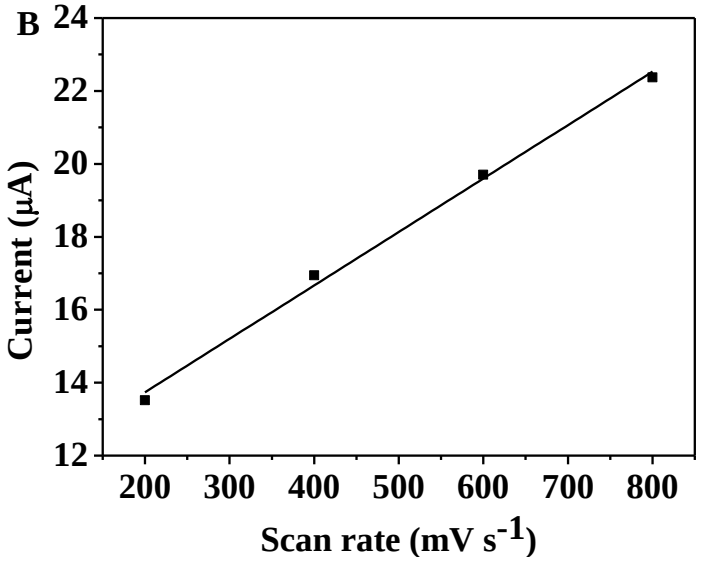

Figure 4. (A) Cyclic voltammetry curves of Tyr-Chi/GC electrode in 50 mmol L^{-1} PBS at scan rates of 200, 400, 600, 800 mV s^{-1}. (B) Plot of anodic peak currents versus scan rates.

The large surface area and superior conductivity of GP-Co_3O_4 nanocomposite provided mounting of favorable sites for electron transfer. Subsequently, more tyrosinase molecules on the GP-Co_3O_4-Tyr-Chi/GC electrode could participate in direct electron transfer on electrode.

As shown in Figure 4, the CV curves of GP-Co_3O_4-Tyr-Chi/GC electrode were recorded at different scan rates ranging from 200 to 800 mV s^{-1}. The anodic peak currents increased linearly with the increase of scan rates. It indicated that the electron transfer between tyrosinase molecules and GC electrode was a surface-controlled process and tyrosinase molecules were immobilized onto GC electrode successfully.

3.3 GP-Co_3O_4-Tyr-Chi/GC electrode detection of catechol

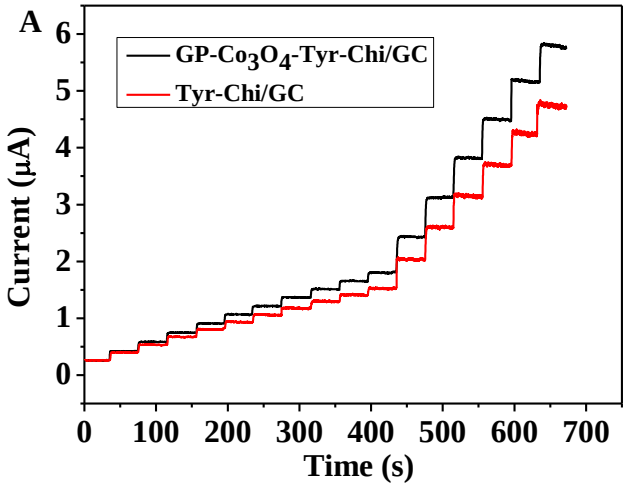

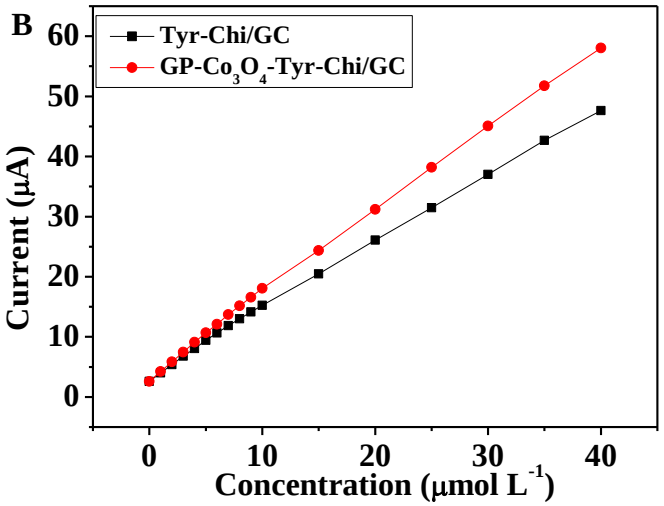

Figure 5. (A) The typical I-T curves of Tyr-Chi/GC and GP-Co_3O_4-Tyr-Chi/GC electrodes with successive addition of 8 μL 1 mmol L^{-1}, 4 μL 10 mmol L^{-1} catechol into stirring 8 mL 50 mmol L^{-1} PBS (pH 6.9). Applied potential: -0.1 V versus Ag/AgCl. (B) The corresponding calibration curves of steady-state currents versus concentrations of catechol: Tyr-Chi/GC and GP-Co_3O_4-Tyr-NGP-Chi/GC electrodes.

Amperometry is a superior sensitive electroanalytical method for the detection of catechol. Through lots of optimization tests of working potential, -0.1 V (versus Ag/AgCl) was considered as the constant working potential because of low LOD and background current. Figure 5A illustrated the typical current-time (I-T) plots of the GP-Co_3O_4-Tyr-Chi/GC and Tyr-Chi/GC biosensors with successive addition of catechol standard solution into stirring 50 mmol L^{-1} PBS (8 mL, pH 6.9). Because the GP-Co_3O_4-Chi/GC biosensor without tyrosinase did not respond to the changes of catechol concentration, the I-T curve did not shown in Figure 5. After the addition of catechol, other biosensors could observe well-defined and fast obvious amperometric signals. This indicated that immobilization tyrosinase molecules on nanocomposite material still possessed their biocatalytic activities. As illustrated in Figure 5B, the calibration curve of GP-Co_3O_4-Tyr-Chi/GC biosensor showed a linear relationship to catechol concentrations in the range of 1 to 30 μmol L^{-1}, LOD of 30 nmol L^{-1}, and sensitivity of 1856.8 mA cm^{-2} M^{-1}. The calibration curve of Tyr-Chi/GC biosensor also illustrated a linear relationship to catechol concentrations from 1 to 30 μmol L^{-1}, LOD of 100 nmol L^{-1}, and sensitivity of 1475.8 mA cm^{-2} M^{-1}. The detection limit of GP-Co_3O_4-Tyr-Chi/GC biosensor was about 20 times lower than that of reported method by Wang's group [27] which developed a polydiphenylamine-4-sulfonic acid (PDPASA, conjugated polymer) and double-stranded DNA (dsDNA) film modified biosensor for analysis of catechol. Nanostructured metal oxides can offer largely effective surface areas for enzyme immobilization and improve the performances of the biosensor through promoting electron transfer between the active site of the desired enzyme and the electrode surface. Qu's group constructed a biosensor incorporating laccase in a ZnO sol-gel with chitosan as a matrix for the determination of catechol. However, its LOD (290 μmol L^{-1}) was also

inferior than that of our reported biosensor [28]. Furthermore, some biosensors were also utilized for catechol detection, but their LOD were not as good as that of GP-Co_3O_4-Tyr-Chi/GC biosensor [29-32]. In summary, these results also indicated that GP-Co_3O_4 nanocomposite material could obviously enhance the sensitivity of only tyrosinase-based biosensor for catechol detection, and its performance were also superior to other biosensors. Thus, the lower LOD of GP-Co_3O_4-Tyr-Chi/GC biosensor could be utilized as a more potential "pre-alarm" tool for rapid detection of catechol on-site.

4. CONCLUSIONS

In the research, an electrochemical tyrosinase biosensor modified on a nanostructured GP-Co_3O_4 nanocomposite material was developed for the detection of catechol. The synergistic effects of the GP-Co_3O_4 nanocomposite material dramatically facilitated direct electron transfer and improved the detection ability of tyrosinase biosensor. In comparison with tyrosinase alone, the nanocomposite material significantly improved the sensitivity of this biosensor. The GP-Co_3O_4 nanocomposite material provided an efficient, robust and universal electrochemical biosensing platform for the fabrication of various enzyme biosensors. It also had a great application prospect for on-site rapid analysis of emergency affairs of catechol.

ACKNOWLEDGEMENT
This work was supported by the National Natural Science Foundation of China (No 21307161), the Special Scientific Research Funds for Central Non-profit Institutes, Chinese Academy of Fishery Sciences (No 2013C006), and Sciencen and technology innovation projects,Chinese academy of agricultural sciences.

References

1. J. Narayanan, M.K. Sharma, S. Ponmariappan, Sarita, M. Shaik, S. Upadhyay, *Biosens. Bioelectron.*, 69 (2015) 249.
2. X.H. Zhang, Q.L. Liao, S. Liu, W. Xu, Y.C. Liu, Y. Zhang, Anal. Chim. Acta., 858 (2015) 49.
3. J.Y. Liu, T.S. Wang, J. Wang, E.K. Wang, *Electrochim. Acta.*, 161 (2015) 17.
4. V. Scherbahn, M.T. Putze, B. Dietzel, T. Heinlein, J.J. Schneider, F. Lisdat, *Biosens. Bioelectron.*, 61 (2014) 631.
5. J.M. Goran, C.A. Favela, K.J. Stevenson, *Acs Cata*l., 4 (2014) 2969.
6. L.D. Wu, X.B. Lu, H.J. Zhang, J.P. Chen, *Chemsuschem.*, 5 (2012) 1918.
7. J.T. Wang, Q.J. Chen, X.J. Liu, W.M. Qiao, D.H. Long, L.C. Ling, *Mater. Chem. Phys*,. 129 (2011) 1035.
8. B. Kalska-Szostko, M. Rogowska, *J. Nanosci. Nanotechno.*, 12 (2012) 6907.
9. C.W. Chuang, J.S. Shih, *Sensor Actuat. B-Chem.*, 81 (2001) 1.
10. M.S. Chang, J.S. Shih, *Sensor Actuat. B-Chem.*, 67 (2000) 275.
11. A. Boujakhrout, A. Sanchez, P. Diez, S. Jimenez-Falcao, P. Martinez-Ruiz, M. Pena-Alvarez, J.M. Pingarron, R. Villalonga, *J. Mater. Chem. B*, 3 (2015) 3518.
12. P. Batalla, A. Martin, M.A. Lopez, M.C. Gonzalez, A. Escarpa, *Anal. Chem.*, 87 (2015) 5074.
13. W. Sun, F. Hou, S.X. Gong, L. Han, W.C. Wang, F. Shi, J.W. Xi, X.L. Wang, G.J. Li, *Sensor Actuat. B-Chem.*, 219 (2015) 331.

14. Y.K. Ye, S. Ding, Y.W. Ye, H.C. Xu, X.D. Cao, S. Liu, H.J. Sun, *Microchim. Acta*, 182 (2015) 1783.
15. Y.H. Pan, L. Shang, F.Q. Zhao, B.Z. Zeng, *Electrochim. Acta*, 151 (2015) 423.
16. F. Gutierrez, F.N. Comba, A. Gasnier, A. Gutierrez, L. Galicia, C. Parrado, M.D. Rubianes, G.A. Rivas, *Electroanal.*, 26 (2014) 1694.
17. H. Beitollahi, S. Tajik, P. Biparva, *Measurement*, 56 (2014) 170.
18. F. Liu, Y. Piao, J.S. Choi, T.S. Seo, *Biosens. Bioelectron.*, 50 (2013) 387.
19. Y.Y. Zhou, L. Tang, G.M. Zeng, J. Chen, J.J. Wang, C.Z. Fan, G.D. Yang, Y. Zhang, X. Xie, *Biosens. Bioelectron.*, 65 (2015) 382.
20. S. Park, A. Singh, S. Kim, H. Yang, *Anal. Chem.*, 86 (2014) 1560.
21. J.Y. Shi, J.B. Guo, G.X. Bai, C.Y. Chan, X. Liu, W.W. Ye, J.H. Hao, S. Chen, M. Yang, *Biosens. Bioelectron.*, 65 (2015) 238.
22. D. Wang, W.H. Hu, Y.H. Xiong, Y. Xu, C.M. Li, *Biosens. Bioelectron.*, 63 (2015) 185.
23. S. Srivastava, M.A. Ali, S. Umrao, U.K. Parashar, A. Srivastava, G. Sumana, B.D. Malhotra, S.S. Pandey, S. Hayase, *Appl. Biochem. Biotech*., 174 (2014) 960.
24. Y.Y. Zhang, M.A. Arugula, M. Wales, J. Wild, A.L. Simonian, *Biosens. Bioelectron.*, 67 (2015) 287.
25. D.H. Deng, L. Yu, X.L. Pan, S. Wang, X.Q. Chen, P. Hu, L.X. Sun, X.H. Bao, *Chem. Commun.*, 47 (2011) 10016.
26. X.B. Lu, G.F. Zou, J.H. Li, *J. Mater. Chem.*, 17 (2007) 1427.
27. P.P. Wang, Y.N. Ni, S. Kokot, *Analyst*, 138 (2013) 1141.
28. J.Y. Qu, T.F. Lou, Y. Wang, Y. Dong, H.H. Xing, *Anal. Lett.*, 48 (2015) 1842.
29. X.H. Yu, J.M. Kong, L.Z. Li, X.J. Zhang, *Chinese J. Anal. Chem.*, 42 (2014) 1400.
30. J.Y. Qu, Y. Wang, J.H. Guo, T.F. Lou, Y. Dong, *Anal. Lett.*, 47 (2014) 2537.
31. S. Singh, D.V.S. Jain, M.L. Singla, *Sensor Actuat. B-Chem.*, 182 (2013) 161.
32. J.Y. Qu, T.F. Lou, S.P. Kang, X.P. Du, *Sensor Lett.*, 11 (2013) 1567.